Monthly groundwater level prediction using ANN and neuro-fuzzy models: a case study on Kerman plain, Iran

Amir Jalalkamali, Hossein Sedghi and Mohammad Manshouri

ABSTRACT

The prediction of groundwater levels in a well has immense importance in the management of groundwater resources, especially in arid regions. This paper investigates the abilities of neuro-fuzzy (NF) and artificial neural network (ANN) techniques to predict the groundwater levels. Two different NF and ANN models comprise various combinations of monthly variablities, that is, air temperature, rainfall and groundwater levels in neighboring wells. The result suggests that the NF and ANN techniques are a good choice for the prediction of groundwater levels in individual wells. Also based on comparisons, it is found that the NF computing techniques have better performance than the ANN models in this case.

Key words | ANN, groundwater level, kerman plain, neuro-fuzzy

Amir Jalalkamali (corresponding author)
Hossein Sedghi
Mohammad Manshouri
Department of Water Sciences and Engineering,
Science and Research Branch,
Islamic Azad University,
Tehran,
Iran
E-mail: *ajalalkamali@yahoo.com*

INTRODUCTION

The estimation accuracy of groundwater levels has an important effect on the efficiency of a supportive deciding system and exploitation from available water resources. Kerman is one of the provinces of Iran which is located in a dry area with 150 mm precipitation on average in a year. Because of the development in cities, industries, agriculture and drought in the two most recent decades, groundwater level has decreased in this area (around 1–3 m in a year). In such a situation, simulated models of groundwater level can be used as an instrument for withdrawing water management from these limited sources. As paying due attention to the gathering of information about the groundwater level takes much time and large costs, it has resulted in the number of information-gathering sites in the area becoming limited. Therefore, the prediction of groundwater levels at other points in the plain was underway without any attention paid to information about soil properties, and the complicated hydraulic water in soil relationships are possible only by use of powerful and careful artificial intelligence (AI) tools. Because of the mentioned reasons, it has been attempted to use models such as artificial neural networks (ANN) and neuro-fuzzy (NF) models for the prediction of groundwater levels by using time series information for the wells around the determined well and climatic time series information.

The AI technique, which is capable of analyzing long series and large-scale data, has increasingly become popular in hydrology and water resources among researchers and practicing engineers in recent years.

Neuro-fuzzy applications in hydrology vary, from real-time to event-based modeling. They have been used for groundwater modeling, level estimation and water quality modeling (Vernieuwe *et al.* 2007; Kholghi & Hosseini 2008; Nourani *et al.* 2008). Dixon (2005) examined the sensitivity of neuro-fuzzy models used to predict groundwater vulnerability in a spatial context by integrating geographic information systems (GIS) and neuro-fuzzy techniques. Nobre *et al.* (2007) calculated nitrate and chloride concentrations using GIS, modeling and a fuzzy logic tool. Neural networks have also previously been applied with success in groundwater level prediction (Daliakopoulos *et al.* 2005; Lallahema *et al.* 2005; Krishna *et al.* 2008).

doi: 10.2166/hydro.2010.034

Bazartseren *et al.* (2003) used neuro-fuzzy and neural network models for short-term water level prediction. Because of the ability of the neuro-fuzzy approach in modeling complex hydrological nonlinear systems, successful applications of this method in water resource modeling have been widely reported, such as flood forecasting (Nayak *et al.* 2004, 2005; Shu & Ouarda 2008). In addition to the above-mentioned points, the neuro-fuzzy and neural network approaches can also predict suspended sediment concentration in rivers (Rajaee *et al.* 2009). Other researchers reported good results in applying ANFIS in hydrological prediction (Cheng *et al.* 2005; Firat & Gungor 2008; Zounemat-Kermani & Teshnehlab 2008; Wang *et al.* 2009). Another study developed the ANN model used to forecast groundwater level changes in an aquifer (Tsanis *et al.* 2008) and ANNs have also been shown to give useful results in many fields of hydrology and water resources research (Campolo *et al.* 2003; Alvisi *et al.* 2006; Wang *et al.* 2008).

But none of the previous publications has provided a comparison for the use of these techniques in the prediction of groundwater levels. Therefore, the major objectives of the study presented in this paper are to investigate two AI techniques for modeling monthly groundwater level prediction, which include ANN approaches and NF techniques.

MATERIALS AND METHODS

Artificial neural networks

The artificial neural network estimation approach has received a great deal of attention from researchers in the last few decades. An interesting property of ANNs is that they often work well even when the training datasets contain noise and measurement errors (Hammerstrom 1993). Moreover, they have the capability of representing complex behaviors of nonlinear systems (Maier & Dandy 2000). The advantage of the ANN is that, with no prior knowledge of the actual physical process and, hence, the exact relationship between sets of input and output data, if acknowledged to exist, the network can be trained to learn such a relationship. The ability to train and learn the output from a given input makes ANNs capable of describing large-scale arbitrarily complex nonlinear problems. A neural network is characterized by its architecture, which represents the pattern of connections between nodes, its method of determining the connection weights and the activation function (Fausett 1994). A typical ANN consists of a number of nodes that are organized according to a particular arrangement. One way of characterizing ANNs is based on the direction of information flow and processing, as feed-forward (where the information flows through the nodes from the input to the output side) and recurrent (where the information flows through the nodes in both directions). Among these combinations, the multi-layer feed-forward networks, also known as multi-layer perceptrons (MLPs), trained with a back-propagation learning algorithm have been found to provide the best performance with regard to input–output function approximation, such as forecasting. As the present study has used an MLP trained with a back-propagation algorithm for the purpose of groundwater level forecasting, the architecture of such a network is described here. A typical MLP with one hidden layer is shown in Figure 1. The first layer connects with the input variables and is called the input layer. The last layer connects to the output variables and is called the output layer. The layer in between the input and output layers is called the hidden layer (there may be more than one hidden layer in an MLP). The processing elements in each layer are called nodes or units. Each of the nodes is connected to the nodes of neighboring layers. The parameters associated with each of these connections are called weights. The architecture of a typical node (in the hidden or output layer) is also shown in Figure 1 (b). Each node j receives incoming signals from every node i in the previous layer. Associated with each incoming signal x_i is a weight w_{ji}. The effective incoming signal s_j to node j is the weighted sum of all the incoming signals:

$$f(s_j) = \frac{1}{1 + \exp^{-s_j}} \quad (1)$$

passing through the effective incoming signal s_j nonlinear activation function (sometimes called a transfer function or threshold function) to produce the outgoing signal (y) of the node. The most commonly used function in an MLP trained with back-propagation algorithm is the sigmoid function. The sigmoid function most often used for ANNs

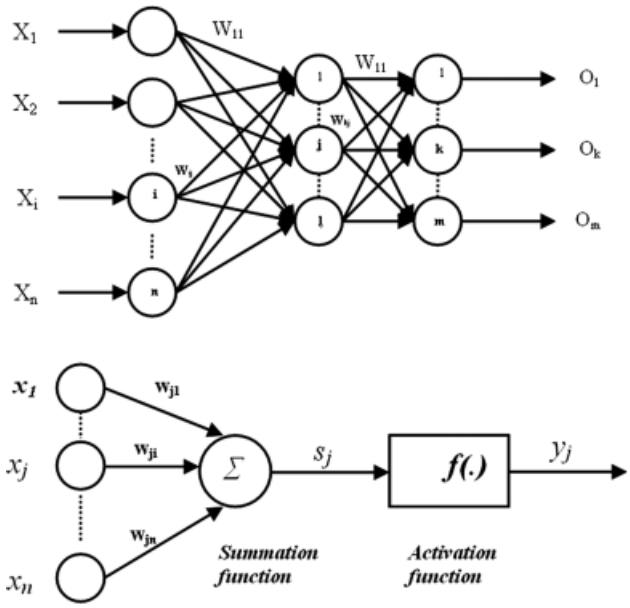

Figure 1 | Typical three-layer feed-forward artificial neural network.

is the logistic function (Sivakumar *et al.* 2002):

$$S_j = \sum_{i=0}^{n} w_{ji} x_i \tag{2}$$

The neuro-fuzzy structure

The ANFIS is a multi-layer feed-forward network which uses neural network learning algorithms and fuzzy reasoning to map inputs into an output. Indeed, it is a fuzzy inference system (FIS) implemented in the framework of adaptive neural networks. As can be seen from Figure 2, the architecture of a typical ANFIS consists of five layers:

For simplicity, a typical ANFIS architecture with only two inputs leading to four rules and one output for the first-order Sugeno fuzzy model is expressed (Sugeno 1985; Wang & Elhag 2008). It is also assumed that each input has two associated membership functions (MFs). It is clear that this architecture can be easily generalized to our preferred dimensions. For a first-order Sugeno fuzzy model, a typical rule set with four fuzzy if–then rules can be expressed as

$$\begin{aligned}
&\text{Rule 1: if } In_1 \text{ is } A_1 \text{ and } In_2 \text{ is } B_1 \text{ then } f_{11} = p_{11}In_1 + q_{11}In_2 + r_{11}\\
&\text{Rule 2: if } In_1 \text{ is } A_1 \text{ and } In_2 \text{ is } B_2 \text{ then } f_{12} = p_{12}In_1 + q_{12}In_2 + r_{12}\\
&\text{Rule 3: if } In_1 \text{ is } A_2 \text{ and } In_2 \text{ is } B_1 \text{ then } f_{21} = p_{21}In_1 + q_{21}In_2 + r_{21}\\
&\text{Rule 4: if } In_1 \text{ is } A_2 \text{ and } In_2 \text{ is } B_2 \text{ then } f_{22} = p_{22}In_1 + q_{22}In_2 + r_{22}
\end{aligned} \tag{3}$$

where A_1, A_2, B_1 and B_2 are labels for representing membership functions for the inputs In_1 and In_2, respectively. Also, p_{ij}, q_{ij} and r_{ij} $(i, j = 1, 2)$ are parameters of the output membership functions which perform different actions in the ANFIS and are detailed below.

Layer 1. All the nodes in this layer are adaptive nodes. They generate membership grades of the inputs. The outputs of this layer are given by

$$\begin{aligned}
O^1_{A_i} &= \mu_{A_i}(In_1), \quad i = 1, 2\\
O^1_{Bj} &= \mu_{Bj}(In_2), \quad j = 1, 2
\end{aligned} \tag{4}$$

where In_1 and In_2 are inputs and A_i and B_j stand for the appropriate MFs, which can be triangular, trapezoidal, Gaussian functions or other shapes. In the current study, the

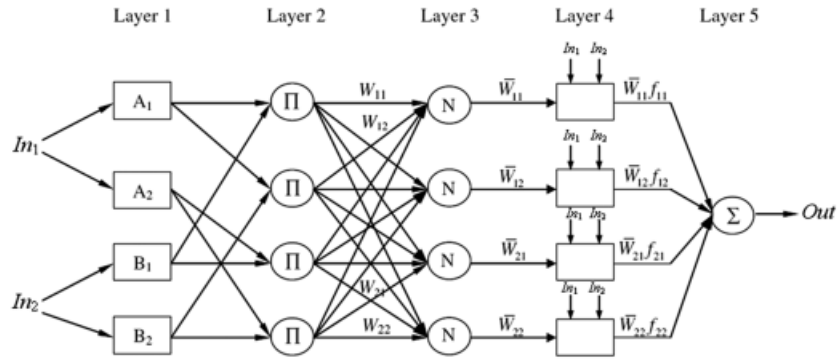

Figure 2 | A typical ANFIS architecture for a two-input Sugeno model with four rules.

Gaussian MFs defined below are utilized:

$$\mu_{A_i}(In_1, \sigma_i, c_i) = \exp\left(-\frac{(In_1 - c_i)^2}{2\sigma_i^2}\right), \quad i = 1,2$$
$$\mu_{B_j}(In_2, \sigma_j, c_j) = \exp\left(-\frac{(In_1 - c_j)^2}{2\sigma_j^2}\right), \quad j = 1,2 \tag{5}$$

$\{\sigma_i, c_i\}$ and $\{\sigma_j, c_j\}$ are the parameters of the MFs governing the Gaussian functions. The parameters in this layer are usually referred to as premise parameters.

Layer 2. The nodes in this layer are fixed nodes labeled Π indicating that they perform as a simple multiplier. The outputs of this layer are represented as

$$O_{ij}^2 = W_{ij} = \mu_{A_i}(In_1)\mu_{B_j}(In_2), \quad i,j = 1,2 \tag{6}$$

Layer 3. The nodes in this layer are also fixed nodes labeled N, indicating that they play a normalization role in the network. The outputs of this layer can be represented as

$$O_{ij}^3 = \overline{W}_{ij} = \frac{W_{ij}}{\sum_{i=1}^{2}\sum_{j=1}^{2} W_{ij}}, \quad i,j = 1,2 \tag{7}$$

They are called normalized firing strengths.

Layer 4. Each node in this layer is an adaptive node, whose output is simply the product of the normalized firing strength and a first-order polynomial (for a first-order Sugeno model). Thus, the outputs of this layer are given by

$$O_{ij}^4 = \overline{W}_{ij} f_{ij} = \overline{W}_{ij}(p_{ij}In_1 + q_{ij}In_2 + r_{ij}), \quad i,j = 1,2 \tag{8}$$

Parameters in this layer are referred to as consequent parameters.

Layer 5. The single node in this layer is a fixed node labeled Σ, which computes the overall output as the summation of all incoming signals, i.e.

$$Out = O^5 = \sum_{i=1}^{2}\sum_{j=1}^{2}\overline{W}_{ij} f_{ij} = \sum_{i=1}^{2}\sum_{j=1}^{2}\overline{W}_{ij}(p_{ij}In_1 + q_{ij}\,In_2 + r_{ij})$$
$$= \sum_{i=1}^{2}\sum_{j=1}^{2}\left[(\overline{W}_{ij}p_{ij})In_1 + (\overline{W}_{ij}q_{ij})In_2 + (\overline{W}_{ij}r_{ij})\right] \tag{9}$$

where the overall output *Out* is a linear combination of the consequent parameters when the values of the premise parameters are fixed.

It can be observed that the ANFIS architecture has two adaptive layers: Layers 1 and 4. Layer 1 has modifiable parameters $\{\sigma_i, c_i\}$ and $\{\sigma_j, c_j\}$ related to the input MFs. Layer 4 has modifiable parameters $\{p_{ij}, q_{ij}, r_{ij}\}$ pertaining to the first-order polynomial. The task of the learning algorithm for this ANFIS architecture is to tune all the modifiable parameters to make the ANFIS output match the training data. Learning or adjusting these modifiable parameters is a two-step process, which is known as the hybrid learning algorithm. In the forward pass of the hybrid learning algorithm, the input membership function parameters are held fixed, node outputs go forward until Layer 4 and the output membership function parameters are identified by the least-squares method. In the backward pass, the output membership function parameters are held fixed, the error signals propagate backward and the input membership function parameters are updated by the gradient descent method. The detailed algorithm and mathematical background of the hybrid learning algorithm can be found in Jang (1993).

Study area and dataset

The area which has been studied in this research is the aquifer of the Kerman plain, which is a part of Kerman province located in the south-eastern of Iran as shown in Figure 3. In this plain, no permanent river exists; therefore, the supply of water demands in the agriculture, industry, domestic and municipal sectors in an area of 3200 km^2 around this plain highly depends on groundwater. Drought and increasing the pumping of wells over the last two decades has been the main cause of groundwater decline, of 1–3 m per year. Furthermore, this problem has caused the decrease of groundwater quality as well. The long-term annual precipitation for the area has noticeably decreased from 150 to 100 mm/yr during the last 20 years (1988–2009).

The data acquired from the area consists of rainfall, temperature and depth of the wells' time series measured at Kerman airport station (latitude: 30°16′ N, longitude: 56°54′ E). The dataset was collected by the Iranian Ministry of Energy (IMOE).

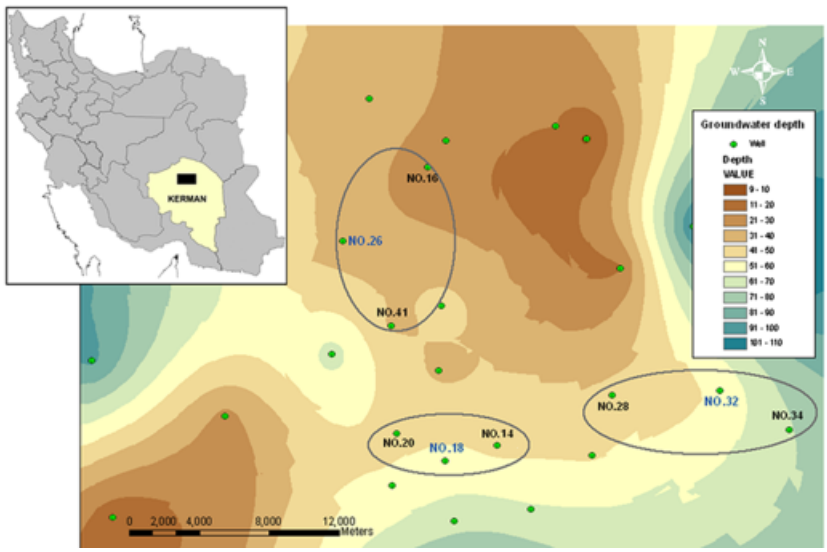

Figure 3 | The location of wells in Kerman plain.

The time series used in this paper are summarized in the following figures. As shown in Figure 4, the monthly precipitation at Kerman airport meteorological station shows the typical characteristics of an arid climate comprised of high rainfall during the winter months. Temperature can also play an important role in the water budget as it affects evapotranspiration. Figure 5 shows the monthly temperature.

The data sample consisted of 22 years (1988–2009) of monthly records of air temperature (T), rainfall (R) and water levels in the target well ($H_{NO.26}$) and neighboring wells ($H_{NO.16}$ and $H_{NO.41}$). The first 19 years (1988–2006) of data were used to train the models and the remaining data were used for testing. The monthly statistical parameters of the data are given in Table 1. In the table X_{mean}, S_x, C_{sx}, X_{max} and X_{min}, respectively, denote the mean, standard deviation, skewness, maximum and minimum.

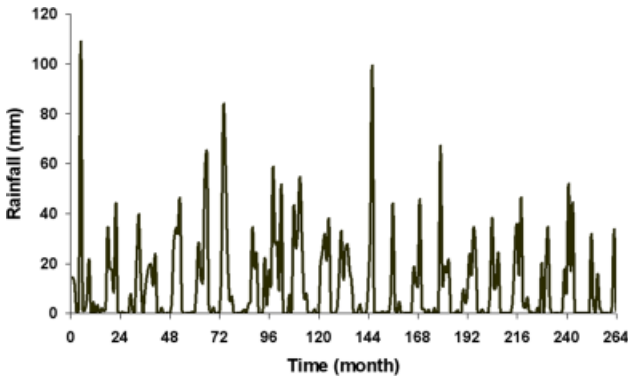

Figure 4 | Time series plot for rainfall versus month.

RESULT AND DISCUSSION

According to recent research (Lalleham *et al.* 2005; Nourani *et al.* 2008), effective factors in the fluctuation of groundwater are temperature, rainfall and water level fluctuation in the nearest lateral piezometers ($H_{NO.16}$ and $H_{NO.41}$) from the target well ($H_{NO.26}$). These characteristics are the major parameters intervening in the mode and the chronology of the piezometric events. By analysing the major parameters, about 15 input combinations were used, from which 4 input combinations gave the best results. Therefore, to reach the best dataset and delay time (t_0 is present time, $t_{0\text{-}1}$ is the monthly lag time and t_{0+1} is the first prediction time step of the well level), the following datasets as input models were shown in Tables 2 and 3. The number of membership functions for the NF model and hidden neurons for ANN was determined by trial and error. Table 2 shows the number of input nodes, membership function (MF) type, number of epochs and number of rules for the NF model. Also Table 3 shows the number of hidden neurons and details of the ANN model for the best architecture of the different models.

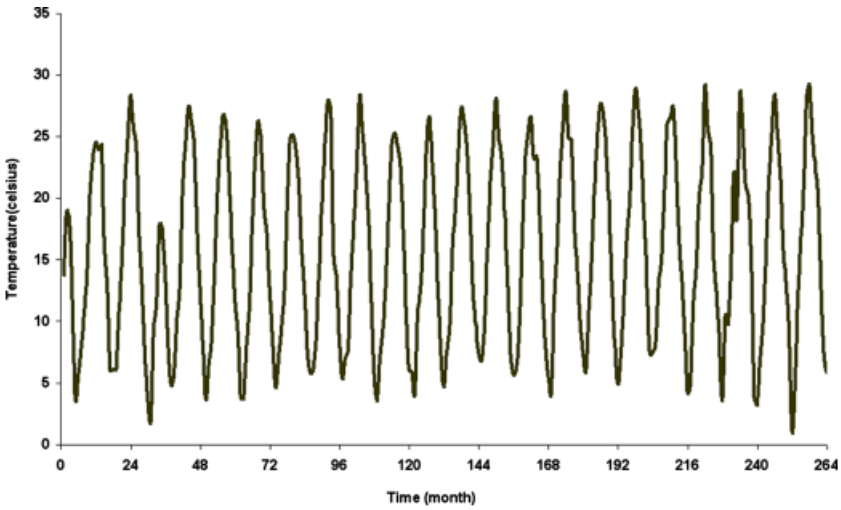

Figure 5 | Time series plot for temperature versus month.

Table 1 | The monthly statistical data parameters

Dataset	Unit	x_{mean}	s_x	c_{sx}	x_{max}	x_{min}
$H_{NO.26}$	m	−33.36	1.74	0.63	−28.82	−35.93
$H_{NO.16}$	m	−37.71	4.3	−0.39	−30.35	−45.49
$H_{NO.41}$	m	−34.57	3.72	0.43	−26.11	−40.53
R	mm	11.26	17.39	2.3	109.1	0
T	°C	15.82	7.68	0.03	29.25	1.05

$$RMSE = \sqrt{\frac{\sum_{i=1}^{n}(H_i^o - H_i^p)}{n}} \tag{10}$$

$$MAPE = \frac{1}{n}\sum_{i-1}^{n}\left|\frac{H_i^p - H_i^o}{H_i^o}\right| \times 100 \tag{11}$$

$$R^2 = \left(\frac{\sum_{i=1}^{n}(H_i^o - \overline{H}_i^o)(H_i^p - \overline{H}_i^p)}{\sqrt{\left[\sum_{i=1}^{n}(H_i^o - \overline{H}_i^o)^2\right]\left[\sum_{i=1}^{n}(H_i^p - \overline{H}_i^p)^2\right]}}\right)^2 \tag{12}$$

Three different types of standard statistics were considered in the statistical performance evaluation. The correlation coefficients (R^2), root mean square error (*RMSE*) and mean absolute percentage error (*MAPE*) were used. The three performance evaluation criteria used in this study can be calculated utilizing the following equations:

where H_i^o is the observed groundwater level at the present time and H_i^P is the predicted groundwater level.

The best fit between calculated values would have been respectively $RMSE = 0$, $MAPE = 100$ and R^2. These statistics of each model in the testing and training period are given in Table 4. This indicates that the NF model whose inputs are

Table 2 | Details of NF model architecture

Row	Input combination	No. of inputs	No. of rules	No. of epoch	MF type
1	$H_{NO.26}(t_0)$, $H_{NO.26}(t_0\text{-}1)$, $H_{NO.16}(t_0)$,$H_{NO.16}(t_0\text{-}1)$, $H_{NO.41}(t_0)$, $H_{NO.41}(t_0\text{-}1)$,$R(t_0)$, $R(t_0\text{-}1)$, $T(t_0)$, $T(t_0\text{-}1)$	10	3	80	gaussmf
2	$H_{NO.26}(t_0)$, $H_{NO.26}(t_0\text{-}1)$, $R(t_0)$,$R(t_0\text{-}1)$, $T(t_0)$, $T(t_0\text{-}1)$	6	3	60	gaussmf
3	$H_{NO.26}(t_0)$, $H_{NO.26}(t_0\text{-}1)$, $H_{NO.16}(t_0)$, $H_{NO.16}(t_0\text{-}1)$, $H_{NO.41}(t_0)$, $H_{NO.41}(t_0\text{-}1)$	6	3	50	gaussmf
4	$H_{NO.26}(t_0)$, $H_{NO.26}(t_0\text{-}1)$, $H_{NO.26}(t_0\text{-}2)$	3	3	50	gaussmf

Table 3 | Details of ANN model architecture

Row	Input combination	No. of inputs	No. of hidden neurons	No. of epoch	Activation function	Network type	Training algorithm
1	$H_{NO.26}(t_0)$, $H_{NO.26}(t_0\text{-}1)$, $H_{NO.16}(t_0)$, $H_{NO.16}(t_0\text{-}1)$, $H_{NO.41}(t_0)$, $H_{NO.41}(t_0 1)$,$R(t_0)$, $R(t_0\text{-}1)$, $T(t_0)$, $T(t_0\text{-}1)$	10	6	300	log-sigmoid	MLP	BP
2	$H_{NO.26}(t_0)$, $H_{NO.26}(t_0\text{-}1)$, $R(t_0)$, $R(t_0\text{-}1)$, $T(t_0)$, $T(t_0\text{-}1)$	6	4	200	log-sigmoid	MLP	BP
3	$H_{NO.26}(t_0)$, $H_{NO.26}(t_0\text{-}1)$, $H_{NO.16}(t_0)$, $H_{NO.16}(t_0\text{-}1)$, $H_{NO.41}(t_0)$, $H_{NO.41}(t_0\text{-}1)$	6	5	200	log-sigmoid	MLP	BP
4	$H_{NO.26}(t_0)$, $H_{NO.26}(t_0\text{-}1)$, $H_{NO.26}(t_0\text{-}2)$	3	4	300	log-sigmoid	MLP	BP

$H_{NO.26}$, $H_{NO.16}$ and $H_{NO.41}$ (input combination number 3) has the smallest *RMSE* (0.019), *MAPE* (0.095) and the highest R^2 (0.95).

Assessing the ability of the NF model compared to the ANN model is represented in Figure 6 in the form of a scatter plot. Also the groundwater level predictions of each model in the testing period for the best input combination are represented in Figure 7 in the form of hydrographs. It is obviously seen from the hydrographs and scatter plots that the NF predictions are closer to the corresponding observed values than the ANN model.

A further analysis was performed in Figure 3 to predict the one-month-ahead groundwater level for the other wells using the best input combination (number 3) in the study area [($H_{NO.18}$) with neighboring wells ($H_{NO.20}$, $H_{NO.14}$) and ($H_{NO.32}$) with neighboring wells ($H_{NO.28}$, $H_{NO.34}$)].

Table 5 shows the goodness-of-fit statistics for each well for both models. Also Table 5 reveals that the NF model may be a good choice for modeling groundwater levels in the one-month-ahead period, especially for this plain.

CONCLUSION

This study is based on the comparative analysis of neural network and neuro-fuzzy systems. In addition, the effect of input combination on model performance was also investigated. The methods used to predict the groundwater level in the Kerman plain in Iran and their performances were evaluated by using *RMSE*, *MAPE* and R^2. It was found that the NF computing technique could successfully be employed in modeling the groundwater level from the available groundwater data.

The main purpose of artificial intelligence (AI) in groundwater applications is that aquifer characteristics, boundary

Table 4 | Error analysis of level prediction in testing and training periods

Set		Training			Testing		
Model	**Input combination**	***RMSE***	***MAPE***	R^2	***RMSE***	***MAPE***	R^2
NF	1	0.064	0.135	0.99	0.126	0.278	0.85
NF	2	0.069	0.150	0.99	0.031	0.158	0.84
NF	3*	0.099	0.199	0.99	0.019	0.095	0.95
NF	4	0.054	0.103	0.99	0.029	0.131	0.85
ANN	1	0.055	0.124	0.99	0.126	0.289	0.83
ANN	2	0.076	0.155	0.99	0.076	0.171	0.87
ANN	3	0.092	0.174	0.99	0.023	0.119	0.92
ANN	4	0.047	0.109	0.99	0.035	0.191	0.84

*Comparing the statistical criteria in testing period, the input combination No.3 is the best

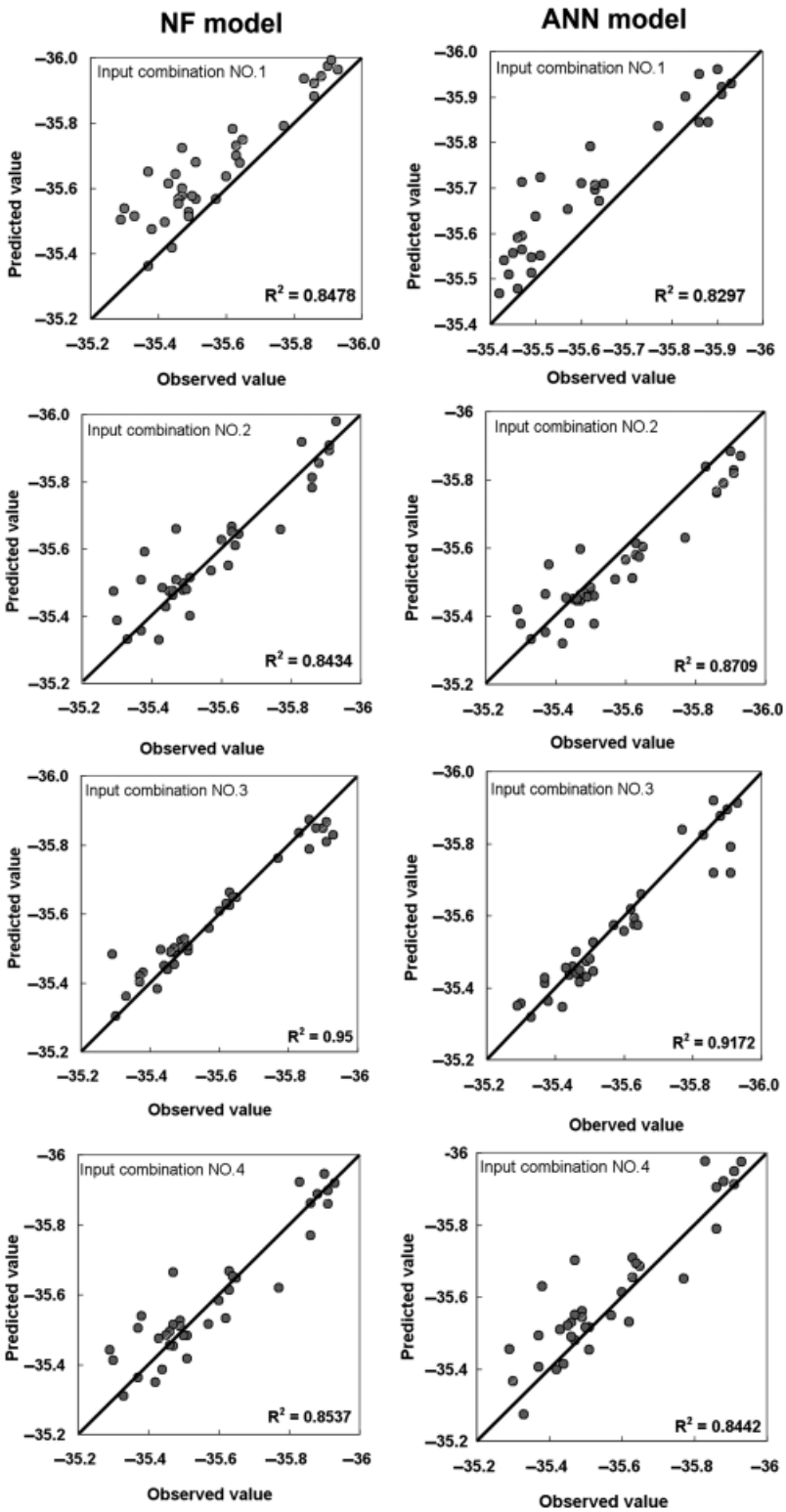

Figure 6 | Scatter plot of the observed and predicted values at testing period for different input combinations.

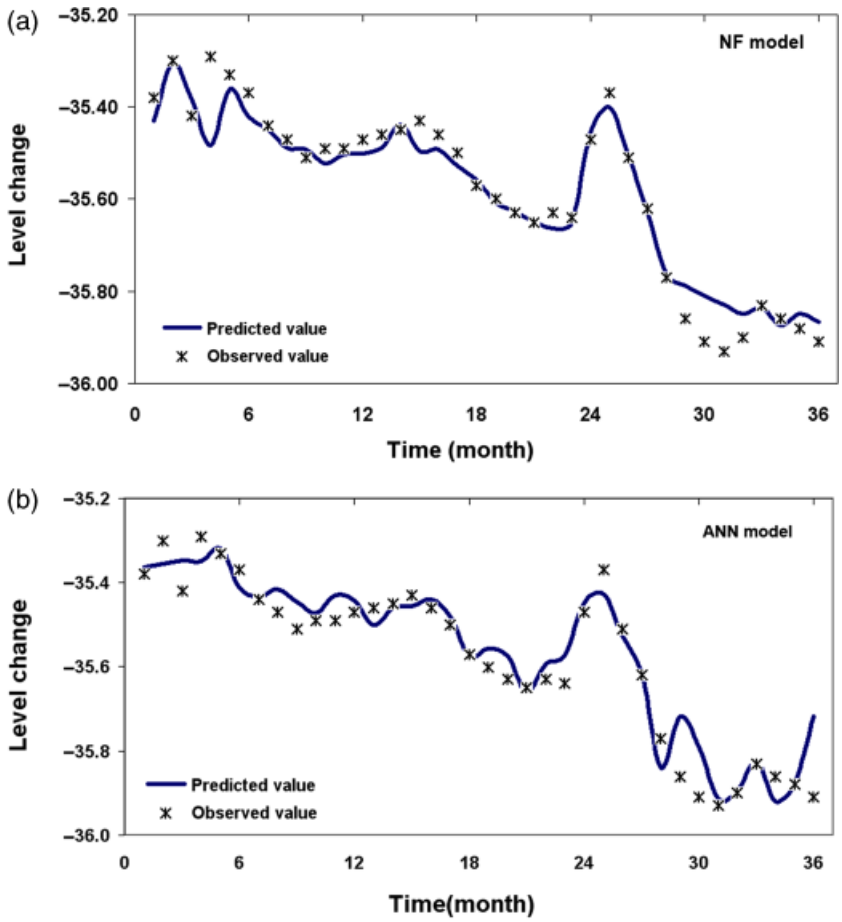

Figure 7 | Observed and predicted level change for the testing period (2007–2009).

and initial conditions might not be required, which are essential in the numerical models. Moreover, the numerical methods also require pumping rates and details of land use/land cover. Information on data pre-processing, determination of suitable input vectors, a systematic way of adopting the optimum architecture and training process with training parameters are needed to understand and assess the applications of the AI models. On the other hand, the black box technology (AI) is only effective for making short-term predictions but physical modeling is appropriate for long-term projections where conditions are expected to change. In general, we can conclude that the AI models were a better

Table 5 | Comparison of performance of models developed for training and testing periods

Set			Training			Testing		
Model	**Well number**	**Input combination**	***RMSE***	***MAPE***	R^2	***RMSE***	***MAPE***	R^2
NF	*NO.18*	3	0.143	0.149	0.98	0.148	0.157	0.98
ANN	*NO.18*	3	0.128	0.151	0.98	0.177	0.245	0.93
NF	*NO.32*	3	0.309	0.496	0.99	0.131	0.205	0.96
ANN	*NO.32*	3	0.276	0.459	0.99	0.276	0.423	0.92

choice for the prediction of groundwater levels in which knowledge of the hydrological parameters is limited. Finally, techniques like support vector machines (SVM) and other faster and stronger ANN algorithms may give better results for groundwater level forecasting in this area.

REFERENCES

Alvisi, S., Mascellani, G., Franchini, M. & Bardossy, A. 2006 Water level forecasting through fuzzy logic and artificial neural network approaches. *Hydrol. Earth Syst. Sci.* **10**(1), 1–17.

Bazartseren, B., Hildebrandt, G. & Holz, K. P. 2003 Short-term water level prediction using neural networks and neuro-fuzzy approach. *Neurocomputing* **55**(3–4), 439–450.

Campolo, M., Soldati, A. & Andreussi, P. 2003 Artificial neural network approach to flood forecasting in the River Arno. *Hydrol. Sci. J.* **48**(3), 381–398.

Cheng, C. T., Lin, J. Y., Sun, Y. G. & Chau, K. W. 2005 Long-term prediction of discharges in Manwan Hydropower using adaptive-network-based fuzzy inference systems models. In: *Advances in Natural Computation, Part 3, Proceedings. Lecture Notes in Computer Science*. Springer-Verlag, Berlin, pp 1152–1161.

Daliakopoulos, I. N., Coulibalya, P. & Tsanis, I. K. 2005 Groundwater level forecasting using artificial neural networks. *J. Hydrol.* **309**, 229–240.

Dixon, B. 2005 Applicability of neuro-fuzzy techniques in predicting ground-water vulnerability: a GIS-based sensitivity analysis. *J. Hydrol.* **309**(1–4), 17–38.

Fausett, L. 1994 *Fundamentals of Neural Networks*. Prentice Hall, Englewood Cliffs, NJ.

Firat, M. & Gungor, M. 2008 Hydrological time-series modelling using an adaptive neuro-fuzzy inference system. *Hydrol. Process* **22**(13), 2122–2132.

Hammerstrom, D. 1993 Working with neural networks. *IEEE Spectrum*. July, 46–53.

Jang, J. S. R. 1993 ANFIS: adaptive-network-based fuzzy inference systems. *IEEE Trans. Syst. Man Cybern.* **23**(3), 665–685.

Kholghi, M. & Hosseini, S. M. 2008 Comparison of groundwater level estimation using neuro-fuzzy and ordinary kriging. *Environ. Model Assess.* **14**(6), 729–737.

Krishna, B., Satyaji Rao, Y. R. & Vijaya, T. 2008 Modelling groundwater levels in an urban coastal aquifer using artificial neural networks. *Hydrol. Process.* **22**, 1180–1188.

Lallahema, S., Maniaa, J., Hania, A. & Najjarb, Y. 2005 On the use of neural networks to evaluate groundwater levels in fractured media. *J. Hydrol.* **307**, 92–111.

Maier, H. R. & Dandy, G. C. 2000 Neural networks for the prediction and forecasting of water resources variables: a review of modelling issues and applications. *Environ. Modell. Software* **15**, 101–124.

Nayak, P. C., Sudheer, K. P., Rangan, D. M. & Ramasastri, K. S. 2004 A neuro-fuzzy computing technique for modeling hydrological time series. *J. Hydrol.* **29**(1–2), 52–66.

Nayak, P. C., Sudheer, K. P., Rangan, D. M. & Ramasastri, K. S. 2005 Short-term flood forecasting with a neuro-fuzzy model. *Wat. Res. Res.* **41**(4), W04004.

Nobre, R. C. M., Rotunno Filho, O. C., Mansur, W. J., Nobre, M. M. M. & Cosenza, C. A. N. 2007 Groundwater vulnerability and risk mapping using GIS, modeling and a fuzzy logic tool. *J. Contam. Hydrol.* **94**, 277–292.

Nourani, V., Mogaddam, A. A. & Nadiri, A. O. 2008 An ANN-based model for spatiotemporal groundwater level forecasting. *Hydrol. Process.* **22**, 5054–5066.

Rajaee, T., Mirbagheri, S. A., Zounemat-Kermani, M. & Nourani, V. 2009 Daily suspended sediment concentration simulation using ANN and neuro-fuzzy models. *Sci. Total Environ.* **407**, 4916–4927.

Shu, C. & Ouarda, T. B. M. J. 2008 Regional flood frequency analysis at ungauged sites using the adaptive neuro-fuzzy inference system. *J. Hydrol.* **349**(1–2), 31–43.

Sivakumar, B., Jayawardena, A. W. & Fernando, T. M. K. G. 2002 River flow forecasting: use of phase space reconstruction and artificial neural network approaches. *J. Hydrol.* **265**, 225–245.

Sugeno, M. 1985 *Industrial Applications of Fuzzy Control*. Elsevier, Amsterdam.

Tsanis, I. K., Coulibaly, P. & Daliakopoulos, I. N. 2008 Improving groundwater level forecasting with a feedforward neural network and linearly regressed projected precipitation. *J. Hydroinf.* **10**(4), 317–330.

Vernieuwe, H., Verhoest, N. E. C., Baets, B. D., Hoeben, R. & Troch, F.P.De. 2007 Cluster-based fuzzy models for groundwater flow in the unsaturated zone. *Adv. Wat. Res.* **30**, 701–714.

Wang, T., Yang, K. L. & Guo, Y. X. 2008 Application of artificial neural networks to forecasting ice conditions of the Yellow River in the Inner Mongolia Reach. *J. Hydrol. Engng.* **13**(9), 811–816.

Wang, W. C., Chou, K. W., Cheng, C. T. & Qiu, L. 2009 A comparison of performance of several artificial intelligence methods for forecasting monthly discharge time series. *J. Hydrol.* **374**, 294–306.

Wang, Y. M. & Elhag, T. 2008 An adaptive neuro-fuzzy inference system for bridge risk assessment. *Expert Syst. Appl.* **34**(4), 3099–3106.

Zounemat-Kermani, M. & Teshnehlab, M. 2008 Using adaptive neuro-fuzzy inference system for hydrological time series prediction. *Appl. Soft Comput.* **8**(2), 928–936.

First received 10 February 2010; 1 May 2010. Available online 28 October 2010